A Full Duplex RF Front End Employing an Electrical Balanced Duplexer and a Chebyshev Load-Balancing Filter

Dror Regev[1], Itamar Melamed[2], Nimrod Ginzberg[2], Emanuel Cohen[2]
[1]Toga Networks, Israel
[2]Faculty of Electrical Engineering, Technion, Israel

***Abstract*— This paper presents a new Chebyshev load-balance (LB) circuit for electrical-balanced RF front-ends targeted for simultaneous transmit-receive (STR) operation. TX reflection of a commercial Wi-Fi antenna with near 3:1 VSWR and direct TX leakage of a commercial quadrature-hybrid are considered and cancelled concurrently in simulations and measurements. We analyze the reflective LB as the RF front-end optimal load and propose a theoretically lossless impedance-matching network that achieves self-interference cancellation (SIC) over more than ± 5 % bandwidth relative to the carrier. A PCB design with two transmission lines and lumped RLC elements is realized to demonstrate the potential of the architecture, achieving > 25 dB of total TX-RX isolation over 300 MHz around 2.65 GHz where the antenna reflection is 7 dBr. This is the first published work that reports cancellation of such a reflective antenna employing a low-cost LB circuit. The proposed Chebyshev LB is theoretically superior to the networks proposed in previous papers.**

***Keywords*— simultaneous transmit receive (STR), full-duplex (FD), transmitter leakage, electrical-balance (EB), duplexer, impedance matching, self-interference cancellation (SIC).**

I. Introduction

The electric-balanced duplexer (EBD) RF Front-End architecture is researched over a decade as an interesting alternative for simultaneous transmit-receive (STR) operation. EBD is known to impose a theoretical 3 dB TX and RX loss. Nevertheless, these losses can be viewed as a TX replica tapping loss for shaping the self-interference cancellation (SIC) signal and the RX loss needed for injecting the SIC signal that nulls the TX leakage. Simple, passive circuits such as transformers or four-port hybrids that can be implemented on chip allow EBD integration and linear designs.

Fig. 1(a) shows an EBD RF Front-End (RFFE) with a transmit input, a receive output, an antenna, and a load-balancer (LB) circuit. The LB is the SIC filter in this topology. Various on-chip lumped LB networks served for EBD in works [1], [2], [3], [4], [5] and [6]. Some of these networks were simply parallel RC terminations, and others included inductors and implemented impedance tuners or transformers. However, the motivation for choosing their respective LB circuit topologies was not detailed. The recent work [7] proposed a frequency division duplex LB and laid out a three-stage circuit with two impedance tuners that enabled TX signal cancellations at the TX and RX frequencies.

While none of the above works proposed cancellation of a real commercial antenna, work [8] utilized an electromechanical tuner and achieved 40 dB of passive TX-RX isolation over 20 MHz at 890 and 1890 MHz.

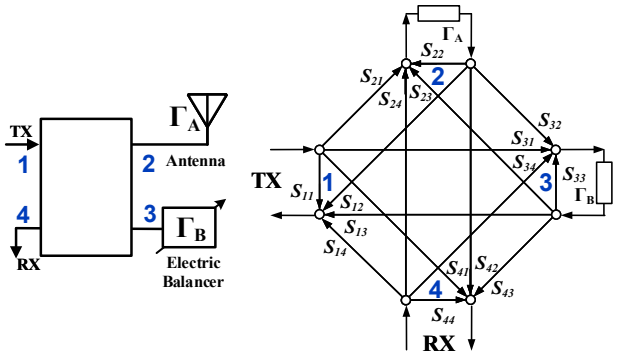

(a) (b)

Fig. 1. Electric-Balance RFFE: (a) schematics; (b) signal flow graph.

In this work, we consider a highly reflective commercial Wi-Fi antenna connected to a commercial quadrature hybrid (QH) and propose a Chebyshev impedance-matching LB design. Chebyshev band-pass filters can theoretically shape a frequency response that can approach the Fano-Bode limit [9] and integrate on a PCB or a chip.

Section II of this article starts with an analysis of a general, passive, 4-port duplexing RFFE. An antenna is connected to the duplexer at the transmit-receive port and an electrical-balancing circuit at the SIC port (see Fig. 1). We first derive a simplified, intuitive expression for electrical-balance TX cancellation at the RX port. Then, we calculate the LB reflection that nulls this leakage. Next, we discuss an RFFE with a practical quadrature hybrid EBD duplexer and provide measurements of commercial Wi-Fi antennas representing the TX-RX leakage considered in this paper.

In section III, we design an optimal RLC Chebyshev 4^{th} order impedance matching LB network. Section IV describes the LB circuit realized in this work and the setup for measurements. Section V concludes this work.

II. TX Leakages and their Cancellation in Electric-Balanced Duplexers

A. TX Self-Interference and Electrical-Balance Cancellation

One can derive the approximated transmit-receive leakage for the duplexer, as shown in Fig. 1(a), by following Mason's analysis [10], utilizing the signal flow graph detailed in Fig. 1(b). A general 4-port S-matrix represents the duplexer,

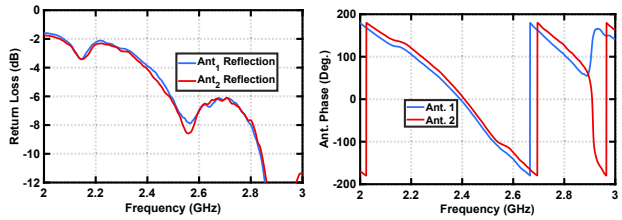

(a) (b)

Fig. 2. TAOGLAS antenna free space reflection: (a) magnitude; (b) phase.

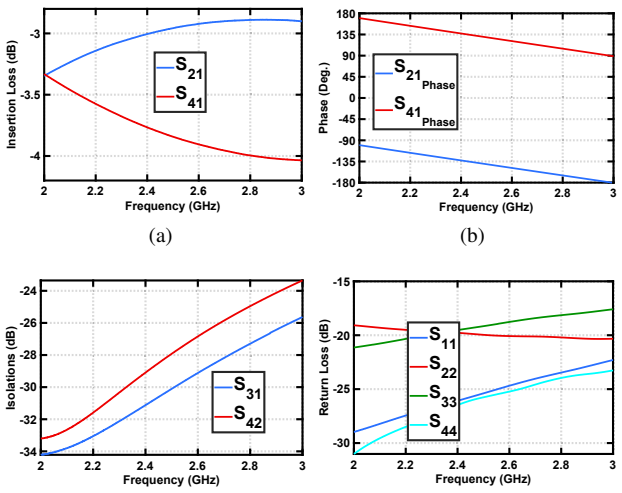

(a) (b) (c) (d)

Fig. 3. ARRA quadrature-hybrid measured performance: (a) insertion loss; (b) transmission phase; (c) isolation; (d) port matching.

and Γ_A and Γ_B, denote the reflection coefficients of the antenna and electrical balancer, respectively. Perfectly matched TX and RX ports are assumed, as well as a reciprocal duplexer with port matching of $S_{22} = S_{33} \leq 0.1$ and isolation values of $S_{23} = S_{32} \leq 0.1$. Under the above simplifications, S_{41_D}, the TX-RX duplexer transfer function is calculated as:

$$S_{41_D} \approx S_{41} + \Gamma_A S_{21} S_{42} + \Gamma_B S_{31} S_{43} \tag{1}$$

The first term in (1) is direct leakage. The second includes the signal portion traveling from the TX port to the antenna Γ_A, which arrives at the RX port. The third represents the load balancer (LB) reflection for a signal traveling towards Γ_B and reflects in the direction of the RX port 4.

To null the TX leakage, and achieve the electrical balance condition, we dictate

$$S_{41_D} = 0 \tag{2}$$

We use the approximated expression of (1) and the reciprocity and symmetry of the quadrature hybrid. Hence, substituting $S_{21}S_{42} = S_{31}S_{43}$, we derive an approximate and simplified, yet intuitive form of the ideal impedance balancer response $\Gamma_{B,ideal}$.

$$\Gamma_{B,ideal,0/90^\circ} \approx -\frac{S_{41}}{S_{31}S_{43}} - \Gamma_A \tag{3}$$

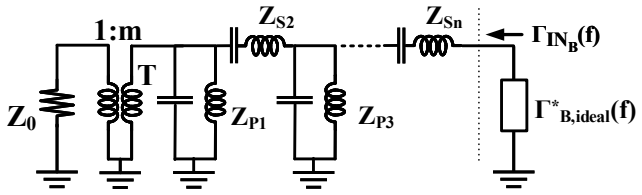

Fig. 4. Chebyshev impedance matching load balancer.

This ideal LB reflection coefficient, cancels self-interference in quadrature hybrid duplexers. It balances both a direct leakage term, as well as an antenna reflection term within the frequency bandwidth (BW) of interest.

B. Commercial Wi-Fi Antenna and Quadrature Hybrid

Expression (3) includes the antenna and the quadrature hybrid performance parameters required for calculating an ideal LB reflection coefficient. A primary design goal was to balance a commercial Wi-Fi antenna; hence, we measured the TAOGLAS FXP830.07.0100C dual-band 2.4-2.5 GHz and 4.9-5.8 GHz dipole connected through a coax cable of 10 cm. Free space reflection coefficient amplitude and phase for the 2-3 GHz BW of two different antenna samples, are shown in Fig. 2(a) and Fig. 2 (b). The measured reflections between 2.4-2.5 GHz are 4-6 dBr and are very difficult to cancel by a load balancer with non-ideal LC components.

The ARRA A4164-90, quadrature hybrid test results are shown in Fig. 3. Insertion losses of 2.8 and 3.9 dB respectively, at 2.7 GHz are shown in Fig. 3(a) and the phases are in Fig. 3(b). Worst case isolation results are better than 24 dB at 3 GHz as shown in Fig. 3(c), and 17 dBr worst case return losses are shown in Fig. 3(d).

C. Load Balancer Design

The input reflection coefficient Γ_B, looking from port 3 of the 4-port duplexer into the electrical balancer circuit as in Fig. 1(a), can be calculated by utilizing [10] and is given by

$$\Gamma_B = S_{11_B} + \frac{S_{21_B} S_{12_B} \Gamma_{B_{OUT}}}{1 - S_{22_B} \Gamma_{B_{OUT}}} \tag{4}$$

where $\Gamma_{B_{OUT}}$ is the reflection coefficient of the LB load. For simplicity of implementation (and calculation), we assume an open circuit as the output of the balancer, hence $\Gamma_{B_{OUT}} = 1$. Moreover, passive LB designs reduce (4) to

$$\Gamma_B = S_{11_B} + \frac{S_{21_B}^2}{1 - S_{11_B}} \tag{5}$$

One can dictate $\Gamma_{B,ideal} = \Gamma_B$, to find the ideal LB S-parameters, S_{ij_B} (i, j $\in$ 1-2), that null Γ_A and the direct leakage of the quadrature hybrid at the RX port

$$S_{11_B} + \frac{S_{21_B}^2}{1 - S_{11_B}} \approx -\frac{S_{41}}{S_{31}S_{43}} - \Gamma_A \tag{6}$$

We treat the design of the LB network as an impedance matching problem in which the source impedance is defined by the conjugate of $\Gamma_{B,ideal}$ (see Fig. 4). Perfect impedance

Table 1. Lumped elements for the lossless Chebyshev $4th$ order load-balancer

f_0	f_{01}	f_{02}	f_{03}	f_{04}
2.65	2.65	2.7	3.57	3.68
R	C_1 L_{01}	L_2 C_{02}	C_3 L_{03}	L_4 C_{04}
121.3	5.67 0.63	21.7 0.17	1.27 1.57	1.7 1.1

1. f_{0n} [GHz]. 2. R [Ω]. 3. C_n [pF]. 4. L_n [nH].

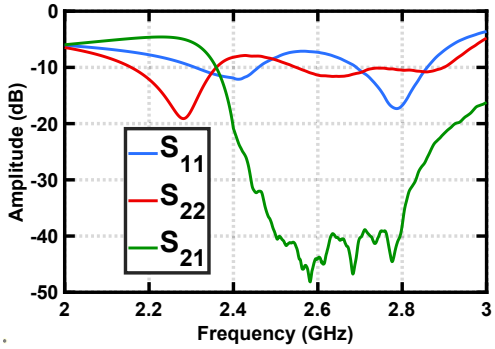

Fig. 5. Simulated SIC performance for the RFFE with a lossless, 4^{th} order Chebyshev load-balancer around 2.65 GHz.

matching will result with an LB that reflects the desired $\Gamma_{B,ideal}$. A Chebyshev impedance matching load balancer implementation, is shown in Fig. 4. This topology enables optimal impedance matching and hence SIC performance [9]. The order of this circuit is defined by the sum of the LC series and parallel resonators that are employed. The Z_0 load and the transformer that transforms its impedance can be substituted by an effective resistor R.

For a real source impedance (real $\Gamma^*_{B,ideal}$), all the LC circuits resonate at ω_0, where

$$\omega_0 = \sqrt{\omega_1 \omega_2} \tag{7}$$

where ω_1, ω_2 are the lower and upper impedance matching frequencies, respectively. LC values are derived as in [9].

Employing lossless networks for impedance matching between a real source and a reactive load is known to be bounded by a fundamental criterion, the Fano-Bode limit [11]. The limit establishes a relationship between the maximum magnitude of the reflection coefficient, as seen by the source into the matching network $\Gamma(\omega)$, and the matched reactive load.

Fano integral bounds take the general form [12]

$$\int_0^\infty g(\omega) \ln \frac{1}{|\Gamma(\omega)|}\, d\omega \leq A \tag{8}$$

where $g(\omega)$ is a weighting function that depends on the transmission zeros of the reactive network of the load when cascaded with the matching network. The constant A, depends on the reactive load and may also relate to the matching network.

Table 2. Circuit elements for the designed load-balancer

f_0	f_{01}		f_{03}	
2.65	2.64		3.81	
R	C_1 L_{01}	d_2 C_2	C_3 L_{03}	d_4 C_4
143.4	1.9 1.5	64.6 0.7	2.2 0.5	47 0.8

1. f_{0n} [GHz]. 2. R [Ω]. 3. C_n [pF]. 4. L_n [nH]. 5. d_n [mm].

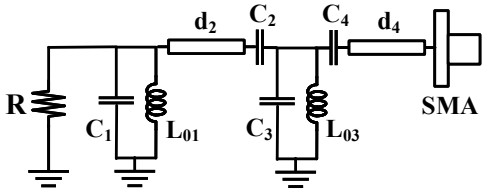

Fig. 6. Schematic of the implenented load balancer.

The choice of a BPF network provides an optimal implementation for the integration limits in (8) since low reflection performance (good matching), is necessary only in-band. In contrast, the reflection coefficient out of the band needs to be high (ideally a full reflection or $|\Gamma(\omega)| = 1$) to set 0 ($\ln\frac{1}{1}$) for the frequencies out of the integration limits. Hence, the area under the integrand in (8) within frequencies ω_1, ω_2, is maximized and $|\Gamma(\omega)|$ is minimized. Conversely, dictating a maximum value for the permissible reflection coefficient, impact the frequency span of the required impedance matching.

III. Chebyshev 4^{th} Order Load-Balancer Design

Band-pass filter impedance matching, can improve as the filter order increases [9]. However, higher-order non-ideal filters lead to higher implementation losses. We chose a 4^{th} order network that can provide the maximum possible bandwidth with SIC of 35-40 dB for the measured antenna. The reactive part of the antenna impedance, interacts with the filter network and needs to be resonated [9]. Therefore, we allowed the two LC sections at the load balncer input to significantly deviate from (7) and partially compensate the antenna. The resonance frequencies of the other two LC sections were also relaxed as

$$\omega_0 \approx \sqrt{\omega_1 \omega_2} \tag{9}$$

Our f_0 frequency for optimization was 2.65 GHz. The resulting lumped elements and section resonance frequencies in our design are summarized in Table I. It is challenging to realize a practical 21.7 nH inductor at 2.65 GHz and accurately realize 0.17 pF. Yet, as shown in Fig. 5, the simulated SIC performance offers a significant bandwidth of operation compared to [8].

IV. Measurements

To realize an LB for measurements, we replaced the series inductors L_2 and L_4 from Table I, with two transmission lines.

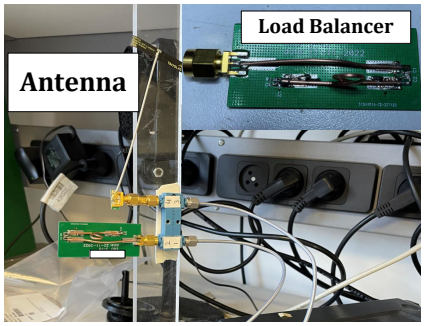

Fig. 7. EBD SIC setup and load-balancer PCB.

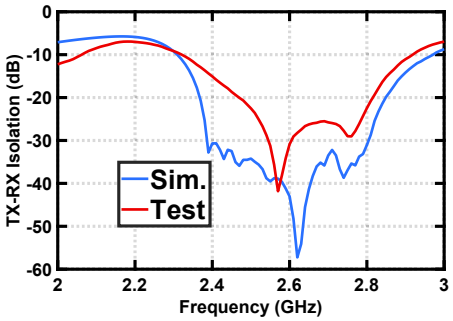

Fig. 8. Simulated versus tested SIC with the designed load balancer.

The LB was designed on a PCB with an SMA connector, and semi-rigid coax cables were utilized to implement the transmission line sections (see Fig. 6). Accordingly, the RLC circuit element values were recalculated. Inductors L_1 and L_3 were selected from the Coilcraft 0402CS series, and the capacitors were from the Murata GRM-15 series. The components' values have a finite resolution that degrades the design flexibility. Also, component parasitics required compensation. Overall, we chose values that imposes little degradation to the performance obtained with the ideal lumped components as in Table I.

The measurements were performed with the antenna TAOGLAS FXP830.07.0100C fixed to a perspex sheet and connected to the ARRA A4164-90 quadrature-hybrid, as shown in Fig. 7. The Perspex sheet skewed the free space antenna performance. Accordingly, we measured the 3-port S-parameters of the quadrature-hybrid connected with the fixed antenna. New circuit optimization was performed to obtain the LC values which nulls the antenna on the Perspex sheet. Table II details the values of circuit elements employed for the LB that was realized.

The setup for final measurements is shown in Fig. 7. In Fig. 8, simulation versus test results are shown, reflecting the LC tolerances and circuit implementation inaccuracies.

Table 3. Comparison Table

	f_0	Antenna	Balancer	SIC BW
[2]	1.95 GHz	50 Ω	40 nm CMOS RC Tunable	50 dB 6 MHz
[4]	2.08 GHz	50 Ω	0.18-μm SOI CMOS RLC 8 bit Tunable	45 dB 230 MHz
[8]	1.89 GHz	Yes 10 dBr	Electromechanical Tuner	40 dB 20 MHz
This work	2.65 GHz	Yes 7 dBr	Chebyshev on PCB Un-Tuned	25 dB 300 MHz

V. Conclusions

In this work, we propose to the convert the SIC design flow into an equivalent impedance matching problem and leverage the respective theories and systematic solutions that were laid out in the past, to achieve an optimal load balance. The proposed Chebyshev topology is theoretically lossless and achieves SIC frequency spans that, to our knowledge, were not reported before. We employ this band-pass filter to cancel the reflection of an antenna with 7 dBr in an electrical-balanced commercial RFFE. Simulations with SMT inductors and capacitors show a potential TX-RX isolation of 30 dB that span 400 MHz around 2.65 GHz. A tunable circuit is desirable and can improve tracking and PVT variations.

References

[1] H. Darabi, A. Mirzaei, and M. Mikhemar, "Highly integrated and tunable rf front ends for reconfigurable multiband transceivers: A tutorial," *IEEE Transactions on Circuits and Systems I: Regular Papers*, vol. 58, no. 9, pp. 2038–2050, 2011.

[2] M. Mikhemar, H. Darabi, and A. Abidi, "A tunable integrated duplexer with 50db isolation in 40nm cmos," in *2009 IEEE International Solid-State Circuits Conference - Digest of Technical Papers*, 2009, pp. 386–387,387a.

[3] S. H. Abdelhalem, P. S. Gudem, and L. E. Larson, "Hybrid transformer-based tunable differential duplexer in a 90-nm cmos process," *IEEE Transactions on Microwave Theory and Techniques*, vol. 61, no. 3, pp. 1316–1326, 2013.

[4] B. van Liempd, B. Hershberg, S. Ariumi, K. Raczkowski, K.-F. Bink, U. Karthaus, E. Martens, P. Wambacq, and J. Craninckx, "A +70-dbm iip3 electrical-balance duplexer for highly integrated tunable front-ends," *IEEE Transactions on Microwave Theory and Techniques*, vol. 64, no. 12, pp. 4274–4286, 2016.

[5] M. Mikhemar, H. Darabi, and A. A. Abidi, "A multiband rf antenna duplexer on cmos: Design and performance," *IEEE Journal of Solid-State Circuits*, vol. 48, no. 9, pp. 2067–2077, 2013.

[6] B. van Liempd, J. Craninckx, R. Singh, P. Reynaert, S. Malotaux, and J. Long, "A dual-notch +27dbm tx-power electrical-balance duplexer," in *ESSCIRC 2014 - 40th European Solid State Circuits Conference (ESSCIRC)*, 2014, pp. 463–466.

[7] K. Shi, H. Darabi, and A. A. Abidi, "Design and analysis of an electrical balance duplexer with independent and concurrent dual-band tx-rx isolation," *IEEE Journal of Solid-State Circuits*, vol. 57, no. 5, pp. 1385–1396, 2022.

[8] L. Laughlin, C. Zhang, M. A. Beach, K. A. Morris, and J. Haine, "A widely tunable full duplex transceiver combining electrical balance isolation and active analog cancellation," in *2015 IEEE 81st Vehicular Technology Conference (VTC Spring)*, 2015, pp. 1–5.

[9] R. Levy, "Explicit formulas for chebyshev impedance-matching networks, filters and interstages," *The Proceedings of the Institution of Electrical Engineers*, vol. 111, no. 6, 1964.

[10] S. J. Mason, "Feedback theory-some properties of signal flow graphs," *Proceedings of the IRE*, vol. 41, no. 9, pp. 1144–1156, 1953.

[11] D. M. Pozar, "Microwave engineering," 2011.

[12] R. Fano, "Theoretical limitations on the broadband matching of arbitrary impedances," *Journal of the Franklin Institute*, vol. 249, no. 1, pp. 57–83, 1950. [Online]. Available: https://www.sciencedirect.com/science/article/pii/0016003250900068